Cellular and Molecular Biology™ **42** (4), 501-509
Printed in France.

0145-5680/96
1996 Cell. mol. Biol.™

DETERMINATION OF MOTILITY FORCES OF HUMAN SPERMATOZOA USING AN 800 NM OPTICAL TRAP

Karsten KÖNIG[1✉,2], Lars SVAASAND[2,3], Yagang LIU[2,4], Greg SONEK[2,4], Pasqualle PATRIZIO[5], Yona TADIR[2], Michael W. BERNS[2] and Bruce J. TROMBERG[2]

[1,✉] Institute of Anatomy II, Friedrich Schiller University, Teichgraben 7, D-07743 Jena, Germany
[2] Beckman Laser Institute and Medical Clinic, University of California, Irvine 92715 CA, USA
[3] Norwegian Institute of Technology, University of Trondheim, N-7034 Trondheim, Norway
[4] Dept. of Electrical and Computer Engineering, University of California, Irvine 92715 CA, USA
[5] Dept. of Obstetrics and Gynecology, University of California, Irvine 92715 CA, USA

Accepted May 10, 1996

Abstract - The measurement and calculation of trapping forces on ellipsoidal specimens, and the determination of intrinsic motility forces of human spermatozoa by employing an 800 nm optical trap ("laser tweezers"), are presented. ATP-driven motility forces were calculated from calibrated trapping forces generated during the interaction of an 800 nm laser beam with single sperm cells. Calibration was performed by moving optically trapped sperm heads through a laminar fluid and calculating viscous forces for an ellipsoidal cell shape. Sperm heads were obtained by microsurgically removing flagellum with a pulsed laser beam ("laser scissors"). A trapping efficiency of 0.12 ± 0.02 and a mean intrinsic motility force of 44 ± 20 pN were determined for motile spermatozoa from healthy donors.

Key words: Laser tweezers, optical trap, laser scissors, motility force, spermatozoa

INTRODUCTION

Interaction of focused laser beams with micrometer-sized particles, such as biological cells, results in momentum change and therefore, in force generation. Change in momentum may occur due to reflection on the outer cell membrane, intracellular scattering, beam refraction and absorption. In addition, absorption-dependent intracellular heating may result in thermal forces caused by intra- and extracellular thermal convection.

Cells generally do not contain efficient endogenous molecular absorbers in the near-infrared (NIR, 700-1300 nm) spectral region. As a result, the net force in the case of a highly focused NIR laser beam is determined primarily by beam refraction. This force F, also called trapping force, can be sufficient to confine and to manipulate a single cell in the focal volume of the objective (single beam gradient force optical trap) (Ashkin, 1970; Ashkin *et al.*, 1986; Ashkin and Dziedzic, 1987). The net trapping force can be represented by:

$$F = Q\frac{P}{c} \qquad (1)$$

where c is the velocity of light in medium, P the incident laser power at the sample, and Q the trapping efficiency parameter with values between 0 and 2. Values of Q equal to 0, 1 and 2 represent, respectively, no interaction, total absorption and total back-reflection of the beam. The one to one correspondence between force and laser power enables the use of optical traps in force measurements. Such force transducers were used to determine the com-

pliance of the rotary motor located in bacteria flagellum (Block *et al.*, 1989), forces for organelle transport (Ashkin *et al.*, 1990), forces exerted by kinesin (Kuo and Scheetz, 1993; Svoboda *et al.*, 1993) and to study the elastic properties of DNA (Chu, 1991; Perkins *et al.*, 1994a, 1994b).

One of the most significant problems with force calculations using optical traps is obtaining a proper calibration. In the case of spherical cells, F can be determined from the Stokes equation by calculating the drag force, F_{drag}, that is exerted when the trapped sample is moved with the maximum (drop off) velocity v_{max} through the medium:

$$F = F_{drag} = 6\pi r \mu v_{max} \qquad (2)$$

where r and μ are, respectively, the radius of the sphere and the dynamic viscosity of the medium. Human spermatozoa are not spherical.

In this paper we present a model which considers the impact on an ellipsoidal geometry on trapping efficiency and viscous force. Model and measurement are combined to determine trapping forces and intrinsic motility forces of single human spermatozoa.

MATERIALS AND METHODS

Experimental Set-up

Optical trapping was carried out by using a modified invert microscope (CLSM, Axiovert 135M, Zeiss, Germany) equipped with a motorized specimen stage. The stage operated in the trapezoid mode with variable, progammable step width, maximum velocity and acceleration (Fig. 1). The trapping beam was provided by an Ar^+-ion laser pumped, broadband cw Ti:Sapphire ring laser (899-01, Coherent, CA). The parallel beam was expanded to fill the back aperture of a 100 x Zeiss Neofluar brightfield objective (440480, immersion oil Zeiss 518C with refractive index n=1.51, numerical aperture NA=1.3). A trapping wavelength of 800 nm was selected since this wavelength permits sperm micromanipulation for more than 10 min. without cell damage, in contrast to shorter-wavelength trapping radiation (König *et al.*, 1995). The set-up was used to determine longitudinal forces (perpendicular to the optical axis).

Additionally, the fundamental wavelength, the second-, or the third harmonics (SHG, THG generation with KDP crystal) of a Q-switched Nd:YAG laser (pulse length: 4-6 ns, Surelite 1, Continuum, Santa Clara, CA; polarizing attenuator: Karl Lambrecht Coop., Chicago, IL) was coupled into the microscope. The SHG radiation (532 nm, pulse energy about 1 mJ) were used in this study for flagellum removal ("laser scissors").

Cell manipulations were monitored with "white" radiation of the halogen lamp (brightfield microscopy) and recorded with a cooled color video camera (ZVS-47DEC, Zeiss).

Determination of in situ Power

Measurements of NIR beam power are typically performed in air after transmission trough the objective. These values are different from the actual power at the sample (in situ power) due to the fact that different refractive indices are encountered as the beam propagates through immersion oil, glass and media during trapping. In addition, power meters are generally not designed for measurement of highly convergent beams. In order to determine the correction factors, we designed a system for obtaining air-measurement correction factors. A microchamber was sandwiched between two identical Zeiss brightfield objectives (100 x, oil, NA= 1.3, working distance: about 240 µm). As shown in fig. 2, the objectives were aligned in such a way that a parallel beam entering the first objective was focused in the center of the chamber. The focal spot of the second objective was adjusted to coincide with that of the first objective resulting in a parallel beam leaving the set-up. In the case of a non-expanded laser beam with a diameter, a, of about 1 mm (beam waist diameter: 0.6 mm, divergence: 1.7 mrad), the total system transmission was measured at 33.9%. Assuming that both objectives have the same transmittance, the transmission for each half of the set-up (objective, oil, glass, and water) is in the case of a non-expanded laser beam: $T_1 = T_2 = (0.339)^{0.5} = 0.582$. However, non-expanded laser beams cannot be focused to the minimum diffraction-limited spot size d. In another experiment, the NIR beam therefore was expanded to $a_1 = 7$ mm that corresponds to the beam diameter in the microscope before entering the objective. Under these conditions total system transmission was determined to be 0.188. The diameter, a_2, of the parallel beam after the second objective was less than a_1, indicating that a part of the incoming beam was obstructed by internal apertures of the first objective. Assuming that T_2 is independent of a_1 (i.e. 1 mm or 7 mm), T_1 will be 0.188/0.582 = 0.323. In contrast, the transmission measured after the first objective (in air, no chamber) was 0.559 for the non-expanded beam, and 0.212 for the expanded laser beam. Since our micromanipulation experiments employed an expanded laser beam, *in situ* NIR powers were determined by multiplying values of measurements in air by the empirically-derived correction factor: $0.323/0.212 \approx 1.5$.

Sperm Cell Preparation

Semen specimens were obtained from three donors with normal semen parameters according to the World Health Organization guidelines (WHO, 1994). Semen was layered on a discontinuous isotonic percoll gradient (Pharmacia,

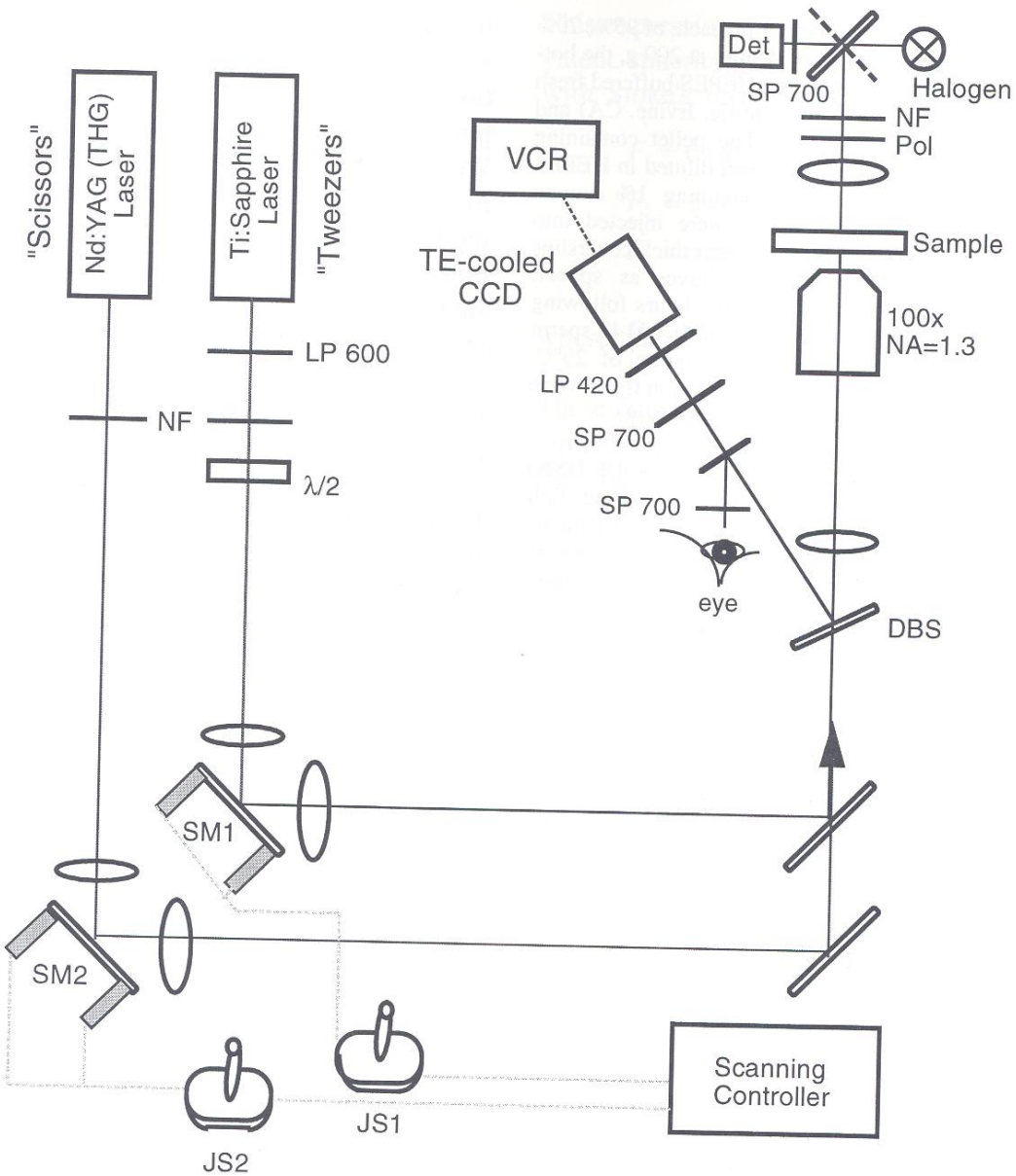

Fig. 1 *Experimental set-up.* A microscope with motorized specimen stage was equipped with trapping- and cutting laserbeams for micromanipulation of optically-trapped motile spermatozoa. A cooled CCD-camera was used for brightfield imaging. NF: neutral density filter; SP: short pass filter; Pol: polarizer; DBS: dichroic beamsplitter; BE: beam expander.

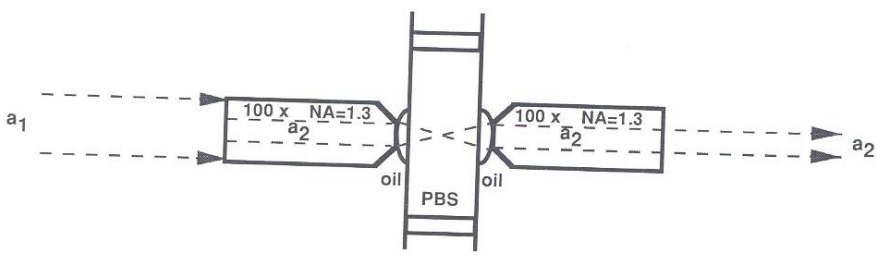

Fig. 2 *Set-up for measurement of objective transmission.* The working distance of the objectives is about 240 µm, the thickness of the coverslip 0.16 µm; a_1 and a_2 are the beam diameters before and after transmission.

Sweden), consisting of three layers, 1 ml each, of 95%, 70% and 50%. After centrifugation for 15 min. at 200 g, the bottom layer was removed, washed with HEPES buffered fresh human tubal fluid (HTF, Irvine Scientific, Irvine, CA) and centrifuged for 10 min. at 100 g. The pellet containing sperm utilized for experiments was then diluted in HEPES buffered isotonic saline solution containing 1% human serum albumin (HSA). Spermatozoa were injected into microchambers consisting of two 0.16 mm thick coverslips separated by a 0.5 mm thick tape layer as spacer. Experiments were performed within three hours following ejaculation. Measurements on a total number of 142 sperm cells were carried out at a room temperature of 29°C. Typical flagellar and head dimensions, shown in fig. 3, were 60 x 0.4 x 0.4 μm, and 5 x 3 x 2 μm, respectively.

The relative viscosity of the medium (HEPES + 1% HSA) compared to water was measured using a Falling Ball Viscosimeter (model: #1, glass ball, Gilmont Instruments, Barrington, IL). Since values were basically the same as water (deviation from water: 3 ± 1% at 29°C), we used water density and viscosity in all calculations.

RESULTS

Determination of minimum Trapping Powers

Sperm cells were confined with an 800 nm laser beam of 150 mW power. The cells were raised to a height, h, of 5.0 ± 0.5 μm above the bottom of the glass using the motor-driven z-stage. The error of 0.5 μm considers the fact that by focusing the laser beam deeper in the medium by axially moving the stage over a distance h, the focus and thus the trapped particle will only be moved over a distance $h.n_1/n_2$ (n_1= refractive index of medium, n_2= refractive index of immersion oil) (Hell *et al.*, 1993). The minimum trapping power required to hold the sperm in the optical trap was determined by laser power reduction using neutral density filters. The power at which the sperm escaped from the optical trap defined the minimum trapping power. We trapped 122 cells with initial movement in the plane perpendicular to the optical axis (x,y-plane). In 13 cases a second sperm cell swam in the same trap during the course of the experiment and pushed the first cell out of the trap ("billiard effect") or remained confined with the other sperm in the trap. 9 trapped cells started to rotate about their head in the x,y-plane (mostly counter clock-wise). In general, trapped sperm cells were aligned laterally in the x,y-plane (not axially) and kept the initial direction of movement in the x,y-plane prior to trapping after escape from the trap ("memory effect"). We did not monitor escape in axial direction nor in the backward direction (opposite direction of movement prior to trapping). A minimum trapping power of 82 ± 38 mW was determined for the 100 single, non-rotating cells in the trap. The lowest value for a motile sperm was found to be 29 mW, the highest 142 mW. A minimum trapping power for immobile sperm of 0.3 ± 0.1 mW was determined.

In order to estimate the corresponding trapping forces, sperm cells were trapped and the sample chamber was translated over a 2 mm distance along the x-axis by the motor-driven specimen stage. The stage speed was varied in 0.48 mm/s steps using the internal microscope software. The acceleration was kept at a constant value of 9.0 cm/s^2. This means, that for typical velocity values of >1 mm/s, the final speed was achieved in <20 ms. The maximum trapping velocity v_{max} was determined in which the sample could be held in the trap in the presence of a drag force produced by the surrounding medium.

We determined the maximum trapping velocity for sperm cells with 150 mW trapping power. In order to eliminate the influence of the ATP-driven intrinsic forces, the cells were paralyzed using UVA light from a mercury lamp. Before starting the motor-driven translation the sperm was aligned in the direction of stage movement using the joystick (x-direction). We found for 10 cells an average maximum velocity of 0.13 ± 0.03 cm/s.

In order to estimate the influence of the sperm tail on v_{max}, the tail of 10 cells was excised using the highly focused laser beam of a Q-switched Nd:YAG laser at 532 nm. A value for the maximum velocity for the sperm heads of 0.30 ± 0.04 cm/s was determined indicating the significant influence of sample shape on v_{max}.

Calculation of viscous Force on ellipsoidal Specimen

The normal human sperm head has a geometry that better can be approximated with an ellipsoid than a sphere. For an ellipsoidal shape, the drag force on the head can be calculated (Lamb, 1932) with: $F_{drag} = 6\pi R_{eq}\mu v_{max}$, where R_{eq} is a parameter given by the half axis lengths a, b, and c (see Fig. 3). We developed a formula for R_{eq} calculation as follows: The viscous force on a non-spherical specimen, which in general is in another direction than the velocity, can be expressed by

$$F_i = \mu a_{ik} v_k \qquad (3)$$

where F_i and v_k are the components of the force and of the velocity, respectively (Landau and Lifshitz, 1987). The quantity a_{ik} is a symmetric tensor of rank two. The independent components of this tensor are dependent on the ellipsoidal geometry and on the orientation of the coordinate system with respect to the axis of the ellipsoid. The tensor can be transformed to a diagonal form by selecting a coordinate system that coincides with the ellipsoidal axis. The three non-zero components of the diagonalized tensor can, when half axis a, b, c are oriented in respectively in x, y, z direction, be expressed (Lamb, 1932) (λ: integration parameter):

$$a_{11} = 16\pi \frac{1}{\int_0^\infty \frac{d\lambda}{\sqrt{(a^2+\lambda)(b^2+\lambda)(c^2+\lambda)}} + a^2 \int_0^\infty \frac{d\lambda}{(a^2+\lambda)\sqrt{(a^2+\lambda)(b^2+\lambda)(c^2+\lambda)}}}$$

$$a_{22} = 16\pi \frac{1}{\int_0^\infty \frac{d\lambda}{\sqrt{(a^2+\lambda)(b^2+\lambda)(c^2+\lambda)}} + b^2 \int_0^\infty \frac{d\lambda}{(b^2+\lambda)\sqrt{(a^2+\lambda)(b^2+\lambda)(c^2+\lambda)}}} \qquad (4)$$

$$a_{33} = 16\pi \frac{1}{\int_0^\infty \frac{d\lambda}{\sqrt{(a^2+\lambda)(b^2+\lambda)(c^2+\lambda)}} + c^2 \int_0^\infty \frac{d\lambda}{(c^2+\lambda)\sqrt{(a^2+\lambda)(b^2+\lambda)(c^2+\lambda)}}}$$

This expression enables the definition of an equivalent spherical radius expressed in accordance with Stoke's formula for the force on a sphere,

$$F_1 = 6\pi R_{eq,1}\mu v_1$$
$$F_2 = 6\pi R_{eq,2}\mu v_2 \qquad (5)$$
$$F_3 = 6\pi R_{eq,3}\mu v_3$$

where $R_{eq,1} = \frac{a_{11}}{6\pi}, R_{eq,2} = \frac{a_{22}}{6\pi}, R_{eq,3} = \frac{a_{33}}{6\pi}$

These equivalent radii are thus dependent on the direction of the velocity with respect to the axis of the ellipsoid.

Typical half axis values for the human sperm head are a= 2.5 µm, b= 1.0 µm and c= 1.5 µm. Therefore, the equivalent radii for velocity along the a, b and c axis are $R_{eq,1}$ =1.50 µm, $R_{eq,2}$ =1.79 µm, $R_{eq,3}$= 1.66 µm. With a translation along the x-axis and the position of the sperm head along the stream lines, the value R_{eq} for typical human sperm is therefore 1.50 µm ($R_{eq,1}$). It should be noted, that with above formula, R_{eq} can be determined for various sperm shapes and allows the determination of the viscous force in any direction or specimen position. The 3D-plot (Fig. 4) demonstrates relative R_{eq} /c values and their dependence on the relative half axis ratios b/c and a/c.

If we assume that two half axes have the same length, a simplified calculation for the equivalent radius R_{eq} can be found. For an ellipsoid of revolution where b=c and a flow in the direction of the a-axis occurs, the force can be expressed:

$$F = \frac{16\pi\mu v}{\int_0^\infty \frac{d\lambda}{(b^2+\lambda)\sqrt{(a^2+\lambda)}} + a^2\int_0^\infty \frac{d\lambda}{(a^2+\lambda)(b^2+\lambda)\sqrt{(a^2+\lambda)}}} = 6\pi R_{eq}\mu v \qquad (6)$$

where R_{eq} is the equivalent radius for this case.

The relative equivalent radius is shown for a prolate ellipsoid, i.e., a>b in fig. 5. This relationship between the equivalent radius and the axes in the prolate ellipsoid can be approximated with a linear function (see bold curve in Fig. 5). The following expression is optimized for the region 1<a/b<5.

$$R_{eq} = 0.1963a + 0.8037b \qquad (7)$$

With the approximation of a ellopsoid with half axes of same length by taking the average of b and c of a typical human sperm: (1.5 µm+1.0 µm)/^{2}=1.25 µm, R_{eq} yields 1.50 µm which gives exactly the above calculated value for human sperm with 3 different axes.

Determination of intrinsic Motility Force

In order to estimate the trapping force F, we have also to consider the competitive acceleration force F_a (same direction x). In the case of a trapped sample and a surrounding medium of maximal velocity we get:

$$0 = F + F_{drag} + F_a \qquad (8)$$

F_a can be estimated to be in the range of $F_a = V\rho a = 10^{-15}$ N for a sperm volume V = 20 µm^3 (assumed ellipsoidal shape of head and tail: $V_{head} \approx$ 16 µm^3; $V_{tail} \approx$ 5 µm^3), a density ρ of 1000 kg/m^3 (for water and in good approximation also for proteins) and the acceleration a = 90 mm/s^2. The acceleration forces are thus negligible.

The very low Reynolds number R (v_{max}=1 mm/s) = $\rho v_{max} r/\mu = 2x10^{-3}$ (where ρ = 1000 kg/m^3 and µ = 0.0081 poise are, respectively, the density and viscosity of water at 29°C (Swindells *et al.*, 1952), ensures the condition of a laminar flow. However, the proximity of the trapped sperm to the microchamber window has to be considered. The correction factor b can be calculated with (Happel and Brenner, 1991; Svoboda and Block, 1994):

$$\beta = 1/(1-9/16(r/h) + 1/8(r/h)^3 - 45/256(r/h)^4 - 1/16(r/h)^5) = 1.20 \qquad (9)$$

where r/h = 1.5/5 = 0.3. With equation (2), F_{drag} yields: β6πµ x 1.5 µm x (0.78 ± 0.04) cms^{-1} = β (178 ± 9) pN = 214 ± 11 pN for 150 mW trapping power. With formula (1) and F = F_{drag} = β6πµ x 1.5 µm x (0.30 ± 0.04) cms^{-1} = 82 ± 10 pN (150 mW), we obtain a Q-value for sperm heads of Q_h= 0.12 ± 0.02 (c_{medium} = 2.25 x 10^8 ms^{-1}).

Under the assumption of linear swim motion, the intrinsic motility forces of motile human spermatozoa can be calculated by use of the Q-value for human sperm heads and the measured minimum trapping power of 82 ± 38 mW. Because the trapping beam interacts only with the sperm head, the Q-value for intact sperm will be also Q_h. The mean intrinsic force F_{in} of motile human spermatozoa in our sample can therefore according formula (1) and (9) determined to be F_{in} = 1/c x (0.12 ± 0.02) x (82 ± 38) mW = 44 ± 20 pN.

DISCUSSION

The relatively complicated shape of human spermatozoa (ellipsoidal head, mid-piece, and flagellum) makes calibration of trapping forces difficult. As demonstrated via two-photon excited fluorescence with the NIR trapping radiation as excitation source (König *et al.*, 1995), the trapping beam is located in the sperm head. The trapping forces on healthy motile cells are therefore

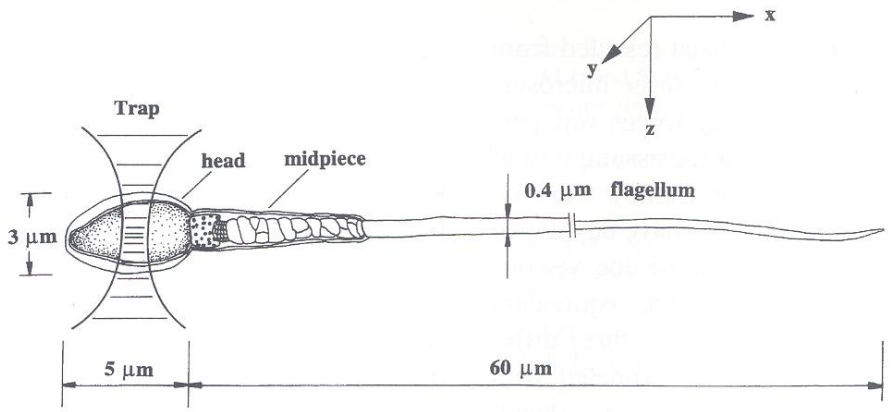

Fig. 3 *Scheme of human sperm cells with typical length parameters.* The trapping beam (z-direction) interacts with the sperm head. In velocity experiments, paralyzed sperm and sperm heads (without flagellum) in the trap were aligned along stream lines in the direction of stage movement (x-direction).

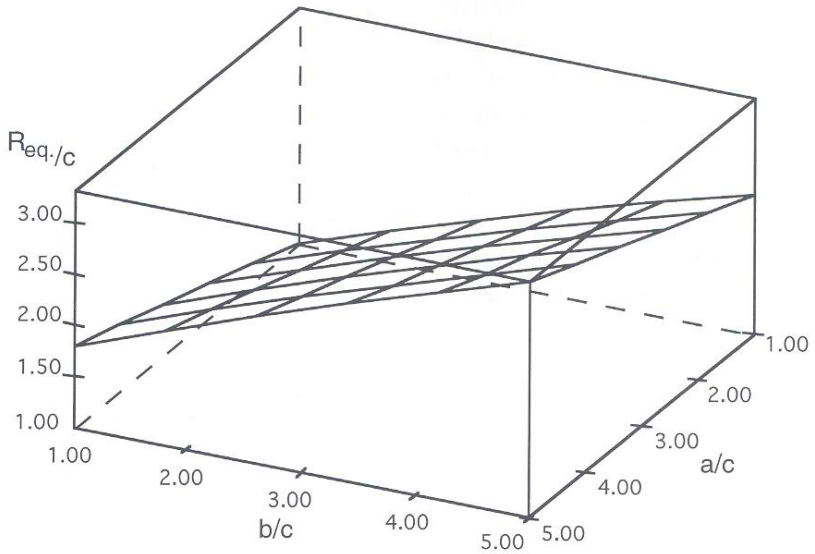

Fig. 4 *Dependence of the relative equivalent radius R_{eq} on half-axis lengths of ellipsoidal specimen.* The 3D-plot shows the relative values R_{eq}/c versus a/c and b/c.

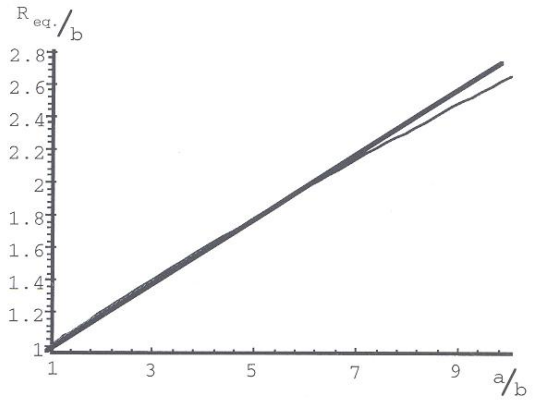

Fig. 5 *Dependence of the relative equivalent radius R_{eq}/b versus relative half axis a/b for prolate rotation ellipsoids with b=c.* For the region 1<a/b<5, the curve can be fitted with $R_{eq}/b=0.1963a/b+0.8037$ (bold line).

the same as the forces on the head resected from the mid-piece and flagellum by laser microsurgery. Calibration of the trapping forces was performed with sperm heads under the assumption of ellipsoidal shape. Based on the Lamb's work on hydrodynamics (Lamb, 1932), we have developed a simplified formula for calculating the viscous force on ellipsoidal specimens. The equivalent radius R_{eq}, for prolate ellipsoids with three different half axis a≠b≠c can be approximated with that of ellipsoids of revolution (b=c). Interestingly, we found an almost linear dependence of the relative equivalent radius R_{eq}/b on the ratio a/b in the range 1<a/b<5 (typical a/b-value for human sperm head: 2). This relation simplifies the force calculation significantly. The calculation gives an equivalent radius, R_{eq}= 1.5 µm, for human spermatozoa. By using this value in the Stokes' Law for an ellipsoid, we are able to determine the trapping efficiency Q.

Our model of intrinsic force calculation using this parameter Q has certain limitations. It bases on the assumption of linear motion of intact sperm cells and neglects the presence of forces in z-direction. As demonstrated by Lighthill (1976), eukaryotic flagellar motions are more complicated and require consideration of undulations (helical movements) and sinusoidal transverse forces, respectively. Our model does also not cover the case that the intact sperm cell exerts forces in transverse direction by a possible twisting and wiggling itself out of the trap. Using (immobile) spheres, the weakest direction of the trap was found in the backward beam direction (Ashkin, 1992). However, we found that in general, trapped motile sperm escaped in the direction of the intrinsic driving force ("memory effect"). Only 8% of the cells (excluded in calculations) lost memory of initial movement direction, started to rotate around beam axis, and escaped in random direction. In the case of the other 92% cells with memory effect, it is still possible that the trapped sperm cell could escape along z-axis or in backward beam direction within one video frame and small displacements on the order of 1 µm which could not be detected. Once free, the sperm could continue its motion in the direction of the intrinsic driving force.

Using the linear model, we determined a mean intrinsic driving force of 44 ± 20 pN for motile sperm cells of healthy donors with the described experimental set-up. In previous studies (Araujo *et al.*, 1994; Dantas *et al.*, 1995) using an 800 nm-trap, minimum trapping powers of 85.1 mW ± 1.2 (n= 1650) (Araujo *et al.*, 1994) and 78.0 ± 43.0 mW (n=1160) (Dantas *et al.*, 1995) for ejaculated sperm, 32.4 ± 1.0 mW (n= 1070) (Araujo *et al.*, 1994) for epididymal sperm, and 76.3 ± 40.0 mW (n=970) for frozen-thawed sperm (Dantas *et al.*, 1995) were determined. No direct force could be calculated at this time. Assuming similar experimental conditions and therefore a similar trapping efficiency parameter Q, our results are in excellent agreement with these high cell number studies and we can calculate mean motility forces of about 18 pN for epididymal spermatozoa and about 45 pN for ejaculated and frozen-thawed sperm.

Baltz *et al.* (1988) determined forces between 110 and 280 pN for human sperm mechanically using a suction micropipette. In this paper, the authors report on extreme difficulties in sperm micromanipulation. In fact, only 15 out of 10,000 investigated motile spermatozoa could be used for force measurements. The authors calculated values of thrust-derived and torque-derived forces of 16 and 190 pN, respectively, and concluded, that the measured force values are due to torque-derived forces, where the flagellum acts as a lever and the edge of the pipette as a fulcrum.

Bonder *et al.* (1990) reported on forces of sea urchin and human sperm of 10-60 pN using optical tweezers. However, they did not consider the non-spherical shape of human sperm. Minimum trapping powers were also determined for human spermatozoa in 760 nm traps (Westphal *et al.*, 1993) and 1064 nm traps (Tadir *et al.*, 1990), but no trapping efficiency parameter was determined. Our results demonstrate the potential of optical

traps as non-contact sterile tools in force measurements even for non-spherical samples, such as human sperm cells. At present, all sperm motility tests are either descriptive, i.e. motility patterns, or velocity determination (in µm/s or degree of forward progression, i.e. +1, ..., +4). Having a more accurate method of intrinsic force determination in absolute terms, possibly in an automated system, may improve our understanding of sperm motility, energy consumption, effects of chemicals on motility and fertilizing capacity.

REFERENCES

Ashkin, A., Acceleration and Trapping of particles by radiation pressure. *Phys. Rev. Lett.* 1970, **24**: 156-159.

Ashkin, A. and Dziedzic, J.M., Optical trapping and manipulation of viruses and bacteria. *Science* 1987, **235**: 1517-1520.

Ashkin, A., Dziedzic, J.M., Bjorkholm, J.E. and Chu, S., Observation of a single-beam gradient force optical trap for dielectric particles. *Opt. Lett.* 1986, **11**: 288-290.

Ashkin, A., Schultze, K., Dziedzic, J.M., Euteneuer, U. and Schliwa, M., Force generation of organelle transport measured *in vivo* by an infrared laser trap. *Nature* 1990, **348**: 346-348.

Ashkin, A., Forces of a single-beam gradient laser trap on a dielectric sphere in the ray optics regime. *Biophys. J.* 1992, **61**: 569-582.

Araujo, E., Tadir, Y., Patrizio, P., Ord, T., Silber, S., Berns, M.W. and Asch, R.H., Relative force of epididymal sperm. *Fert. Steril.* 1994, **62**: 585-590.

Baltz, J.M., Katz, D.F. and Cone, R.A., Mechanics of sperm-egg interaction at the zona pellucida. *Biophys. J.* 1988, **54**: 643-654.

Block, S.M., Blair, D.F. and Berg, H.C., Compliance of bacterial flagella measured with optical tweezers. *Nature* 1989, **338**: 514-518.

Bonder, E.M., Colon, J.M., Dziedzic, J.M. and Ashkin, A., Force production by swimming sperm: analysis using optical tweezers. Am. Soc. Cell Biol., Meeting of 9-13 Dec. 1990, San Diego, In: *J. Cell Biol.* 1990, **111**: abstract-No. 2349.

Chu, S., Laser manipulation of atoms and particles. *Science* 1991, **253**: 861-866.

Dantas, Z.N., Araujo, E., Tadir, Y., Berns, M.W., Schell, M.J. and Stone, S.C., Effect of freezing on the relative escape force of sperm as measured by a laser optical trap. *Fertil. Steril.* 1995, **63**: 185-188.

Happel, J. and Brenner, H. (eds.) *Low Reynolds Number Hydrodynamics.* Kluwer Academic, Dordecht, 1991, p. 553.

Hell, S.W., Reiner, G., Cremer, C. and Stelzer, E.H.K., Abberrations in confocal fluorescence microscopy induced by mismatches in refractive index. *J. Microsc.* 1993, **169**: 391-405.

König, K., Liang, H., Berns, M.W. and Tromberg, B.J., Cell damage by near-IR microbeams. *Nature* 1995, **377**: 20-21.

Kuo, S.C. and Scheetz, M.P., Force of single kinesin molecules measured with optical tweezers. *Science* 1993, **260**: 232-234.

Lamb, H. (ed.), *Hydrodynamics.* 6th ed., Cambridge, 1932, §339.

Landau, L.D. and Lifshitz, E.M., *Fluid Dynamics.* Pergamon Press, Oxford, 1987, §20: 61.

Lighthill, J., Flagellar hydrodynamics. *SIAM Review* 1976, **18**: 161-230.

Perkins, T.T., Smith, D.E. and Chu, S., Direct observation of tube-like motion of a single polymer chain. *Science* 1994, **264**: 819-822.

Perkins, T.T., Quake, S.R., Smith, D.E. and Chu, S., Relaxation of a single DNA molecule observed by optical microscopy. *Science* 1994, **264**: 822-826.

Svoboda, K., Schmidt, C.F., Schnapp, B.J. and Block, S.M., Direct observation of kinesin by optical trapping interferometry. *Nature* 1993, **365**: 721-727.

Svoboda, K. and Block, S.M., Biological applications of optical forces. *Annu. Rev. Biophys. Biomol. Struct.* 1994, **23**: 247-285.

Swindells, J., Coe, R. and Godfrey, T.B., *J. Res. National Bureau of Standards* 1952, **48**: 1.

Tadir, Y., Wright, W.H., Vafa, O., Ord, T., Asch, R.H. and Berns, M.W., Force generated by human sperm correlated to velocity and determined using a laser generated optical trap. *Fertil. Steril.* 1990, **53**: 944-947.

Westphal, L.M., El Dansasouri, I., Shimitzu, S., Tadir, Y. and Berns, M.W., Exposure of human spermatozoa to the cumulus oophoruse results in increased relative force as measured by a 760 nm laser optical trap. *Human Reprod.* 1993, **8**: 1083-1086.

World Health Organization, *WHO Laboratory Manuel for the Examination of Human Semen and Semen-Cervical Mucus Interaction.* 3d ed. Cambridge University Press, Cambridge, 1994.